Available online at www.sciencedirect.com
ScienceDirect
Polymer 48 (2007) 5662–5670
polymer
www.elsevier.com/locate/polymer

# The effect of interfacial chemistry on molecular mobility and morphology of multiwalled carbon nanotubes epoxy nanocomposite

Mohamed Abdalla [a], Derrick Dean [a,*], David Adibempe [b], Elijah Nyairo [c], Pamela Robinson [d], Gregory Thompson [e]

[a] *University of Alabama at Birmingham, Department of Materials Science and Engineering, Birmingham, AL 35294-4461, USA*
[b] *Think Tank Innovations, Baltimore, Maryland, USA*
[c] *Alabama State University, Department of Physical Science, Montgomery, AL 36101, USA*
[d] *Tuskegee University, Department of Chemistry, Tuskegee, AL 36088, USA*
[e] *University of Alabama, Department of Metallurgy and Materials Engineering, Tuscaloosa, AL 35487, USA*

Received 29 May 2007; received in revised form 28 June 2007; accepted 30 June 2007
Available online 15 July 2007

**Abstract**

We report on our attempts to understand the link between the nature of the CNT surface modification, dispersion in an epoxy resin and the resulting properties. Carboxylated and fluorinated nanotubes were used to synthesize nanocomposites by dispersing them separately in an epoxy resin. Dynamic mechanical analysis, using torsional deformation, was applied both parallel and perpendicular to the long axis of the multiwall nanotubes (MWNTs). Interestingly, for epoxy/MWNT (1 wt%) nanocomposites, the shear moduli in the glassy state were higher for the nanocomposites, and it's highest for the nanocomposites in which the nanotubes are parallel to the direction of applied torque. These nanocomposites also exhibited higher $T_g$s than the neat resin. In addition, the rubbery plateau modulus (between 150–200 °C) was higher by a factor of three for the nanocomposites. Master curves constructed using time–temperature superposition allowed us to probe low frequency dynamic moduli and further discern differences in the relaxation behavior. Samples containing fluorinated nanotubes exhibited the highest $T_g$s, longest relaxation times and highest activation energies relative to the carboxylated nanotube samples and the neat resin, indicative of stronger interactions. SEM and TEM studies confirmed the nanotube dispersion and alignment.


*Keywords:* Carbon nanotubes; Epoxy nanocomposite; Rheology

## 1. Introduction

Nanocomposites based on carbon nanotubes (CNTs) have received a tremendous amount of attention during the past five to ten years. Much of the excitement is due to the interesting set of properties that CNTs can exhibit, including moduli on the order of 1 TPa, strength of 50–200 GPa, failure strains of up to 15% and electrical conductivity ranging from semiconducting to metallic, depending on their structure [1–4]. Potential applications of polymer/CNT nanocomposites are numerous, including aerospace and automotive materials (high temperature and light weight), optical switches, EMI shielding, photovoltaic devices, packaging (films and containers), adhesives and coatings. However, the foundations for harnessing the wealth of physics present within nanotube structures hinge on the ability to optimize the dispersibility of nanotubes in solution. To tackle the dispersibility issue, surface modification has been used to effect homogeneous dispersibility and spatial distribution of CNTs in host materials [1–11].

Thermoset polymers comprises of a broad range of polymers with a large number of industrially relevant applications, including coatings, encapsulants and matrices for fiber reinforced

* Corresponding author. Department of Materials Science and Engineering, University of Alabama at Birmingham (UAB), 1530 3rd Avenue, South, Birmingham, AL 35294-4461, USA. Tel.: +1 205 975 4666; fax: +1 205 934 8485.
*E-mail address:* deand@uab.edu (D. Dean).

0032-3861/$ - see front matter © 2007 Elsevier Ltd. All rights reserved.
doi:10.1016/j.polymer.2007.06.073

composites. Thus, the idea of combining CNTs with thermosets is very appealing from several perspectives. Several recent studies have reported dispersions of CNTs in thermoset and their resulting physical and mechanical properties [1–12]. In general, the mechanical and physical properties such as electrical conductivity were found to depend on the degree of dispersion of the CNTs. Control of the nanotube dispersion can be facilitated by manipulating the polymer-CNT interface. This can be accomplished via either primary or secondary interactions between the CNT and resin. Secondary interactions can occur between certain functional groups attached to the CNT surface and the resin, wrapping a polymer around the nanotube [3,10,12–15], or by using surfactants [2]. While some of these approaches have resulted in enhanced CNT dispersion, it is presumed that covalent interactions will yield the best dispersion and the best properties.

With respect to covalent interactions, a number of studies in which chemical modification have enhanced the nanotube dispersion in the polymer matrix have appeared recently [3–5, 8–11,16,17]. A number of approaches have been used to attach reactive functional groups to the nanotube surface, however, not all of these modified tubes have been integrated into epoxy resins. Among the approaches that have led to successful integration into epoxies is the oxidation of nanotube surface followed by dispersal or further derivatization [16], amine functionalization [5,18], and fluorination [3]. Oxidation of both single and multiwall nanotubes has been reported by several groups [4,19–21]. However, direct evidence of covalent interactions between the modified CNT and epoxies has not been reported. This is presumably due in part to the relatively low concentration of functional groups on the CNT surface when dispersed into the epoxy resin/curing agent mixture, which makes it difficult to pinpoint the reaction. In an attempt to investigate the interfacial reaction, Schadler et al., oxidized multiwall nanotubes (MWNTs) to generate carboxylic acid groups on the surface followed by dispersal in an epoxy resin in the absence of the curing agent [4]. Spectroscopic and thermal analysis verified that a reaction with the epoxy resin diglycidyl ether of bisphenol A (DGEBA) resulted in the formation of covalent bonds. The effects of acid oxidized, amine functionalized and plasma oxidized MWNTs on the rheology and mechanical properties of an epoxy based thermoset were reported by Kim et al. [16]. They found that all of the systems were well dispersed. However, the amine and acid treated nanotubes both yielded similar nanocomposite modulus and strength enhancements relative to the neat resin, while the plasma treated nanotubes yielded a significantly higher strength. No explanation was provided for this difference. However, it may be due to several factors, including a more homogeneous nanotube coating from the plasma leading to better dispersion, and no disruption of the nanotube structure during the modification process. Barrera et al. achieved enhanced mechanical properties and excellent nanotube dispersion in an epoxy matrix using fluorinated single wall nanotubes (SWNTs) [3]. The SWNTs were acid oxidized followed by fluorination and subsequently dispersed in an epoxy resin using a solvent approach. They showed spectroscopically, that both carboxylic acid and fluorine modified nanotubes were grafted onto the tube surface. In addition, they used FT-IR to confirm that covalent bonds were formed when model reactions between the CNTs and amine curing agent were conducted. They concluded that similar reactions occurred in the resin-CNT dispersion.

Clearly, carbon nanotube modification enhances dispersion and the resulting properties. It is not clear, however, how the modified CNTs react with the epoxy resins. The differences in the way the epoxy and/or the amine curing agent reacts with the different nanotube modifications can result in steric and electronic differences that can in turn affect the cure. This invariably translates to differences in the crosslink topology and hence the macroscale properties. These effects need to be understood and corroborated with the state of dispersion. In this paper, we report on our attempts to understand the link between the nature of the CNT surface modification, dispersion in an epoxy resin and the resulting properties. We attempted to show that dynamic mechanical analysis is a very valuable tool for providing insight into the interfacial interactions and their impact on the issues discussed above.

## 2. Experimental

### 2.1. Materials

The EPIKOTE resin EPON 828 and EPIKURE curing agent W were purchased from Miller–Stephenson Company. EPON 828, diglycidyl ether of bisphenol A (DGEBA) epoxy resin and W is a nonmethylene dianiline, aromatic amine curing agent (diethyltoluenediamine). The MWCNTs were purchased from Materials and Electrochemical Research (MER) Corporation. MWCNTs were synthesized by catalytic chemical vapor deposition (CVD) with 35 nm diameter and approximately 30 μm length. The purity of as received MWCNT is greater than 90%, with less than 0.1% metal (Fe) content.

### 2.2. Epoxy/MWCNT synthesis

#### 2.2.1. Chemical treatment

*2.2.1.1. Oxidation of carbon nanotubes.* The CNTs were treated with a mixture of sulfuric/nitric acid, which helped to remove impurities from the surface. A 1 g portion of nanotubes was added to a mixture of sulfuric/nitric acid (3:1 by volume). The mixture was sonicated in a water bath for 3 h at 40 °C. The mixture was then diluted with a 1:5, by volume, distilled water. The CNTs were recovered by filtering the mixture through polycarbonate membrane filter (ATTP 0.8 μm pore size) and washing with an excess of water until no residual acid is present. Finally, the CNTs were dried for 24 h in a vacuum oven. This resulted in –COOH groups on the surface.

*2.2.1.2. Fluorination of carbon nanotubes.* In a flame-dried three necked round bottom flask fitted with a condenser a 1 g of MWCNT, 15 mL 2-methoxyethyl ether, and 3.1 mL

of 4-fluoroaniline were added. The mixture was purged with nitrogen by bubbling it through a needle. While maintaining an inert atmosphere 4 mL of amyl nitrate was added slowly using a dropping funnel. The mixture was stirred at room temperature for 1 h and then the temperature was raised up to 70 °C and mixing was continued for 3 h. The product was cooled, diluted with diethyl ether, filtered and then washed with copious amounts of water. The wet product was dried in vacuum oven for 24 h.

### 2.3. CNT dispersal

A high shear method was used to mix the samples. An appropriate amount of MWCNT was dispersed into the epoxy resin by using an extrusion process. The device used in this process is shown in Fig. 1. The plunger was used to extrude the mixture through syringe 2 into syringe 3. This process was repeated up to 50 times to ensure a good dispersion. The equivalent amount of curing agent was added and mixed using the same process. The dispersed pre-polymer was poured into a steel mold, degassed under vacuum for 20 min, and subsequently cured at 122 °C for 4 h. The sample codes used in this study are listed in Table 1.

### 2.4. Characterization

Dynamic mechanical properties were measured using a rheometer (TA AR2000) in torsion rectangular mode. Temperature scans were made using a strain of 0.1%, an oscillatory frequency of 1 Hz and heating rate of 5 °C min$^{-1}$. TEM samples were prepared by cutting thin slices from the composite using standard microtome techniques and collecting the slices onto a carbon coated grid. A FEI Tecnai F20 Supertwin Transmission electron microscope (TEM) was used to collect micrographs. Scanning electron microscopy micrographs of a freeze fracture surface of nanocomposite samples were taken using a JEOL-7000F. Fourier transform infrared (FT-IR) spectra of carbon nanotube samples were measured with a Nicolet 4700 in transmission mode at room temperature. The carbon nanotubes were mixed with KBr powder and then a KBr disc was made using a die in a Carver press. The resolution for FT-IR was at 4.0 cm$^{-1}$. Raman spectroscopy was carried out using a backscattering geometry. The wavelength of 442 nm line of the Kimmon Electric's HeCd laser was used to excite the sample. The laser beam with a nominal power of 80 mW was focused onto 5 μm diameter spot.

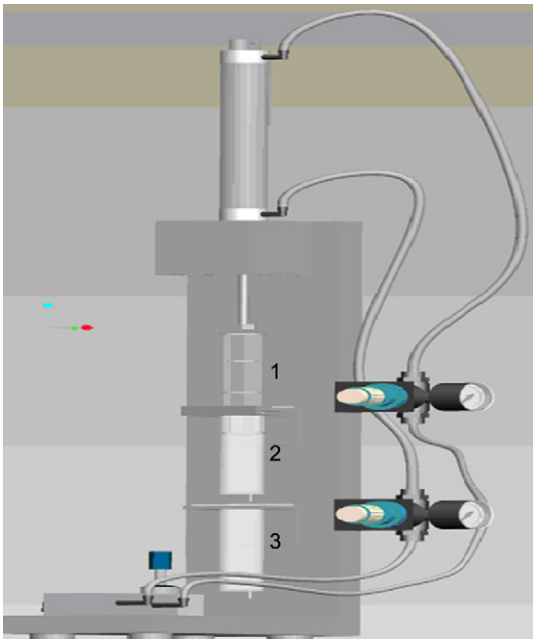


Fig. 1. Schematic of shearing device.

Table 1
Sample codes used in this study

| Sample codes | Description |
|---|---|
| Neat | |
| EPON/1CNTPar | 1 wt% CNT, tested parallel to CNT orientation |
| EPON/1CNTPer | 1 wt% CNT, tested perpendicular to CNT orientation |
| EPON/4CNTPar | 4 wt% CNT, tested parallel to CNT orientation |
| EPON/4CNTPer | 4 wt% CNT, tested perpendicular to CNT orientation |
| EPON/1_F-CNTPar | 1 wt% F-CNT, tested parallel to CNT orientation |
| EPON/1_F-CNTPer | 1 wt% F-CNT, tested perpendicular to CNT orientation |
| EPON/4_F-CNTPar | 4 wt% F-CNT, tested parallel to CNT orientation |
| EPON/4_F-CNTPer | 4 wt% F-CNT, tested perpendicular to CNT orientation |

## 3. Results and discussion

### 3.1. Nanotube characterization

The chemical and structural natures of the nanotubes after modification were characterized using infrared and Raman spectroscopies. FT-IR scans of the samples are shown in Fig. 2. Carboxylic acid functional groups (−COO) were identified on the surface of the oxidized MWCNTs by FT-IR spectroscopy, with similar results to those reported by others [22,23]. Vibrational modes observed, at 3436 cm$^{-1}$ and 1572 cm$^{-1}$, were attributed to O−H stretching and carbonyl stretching, respectively, which did not exist in original nanotubes.

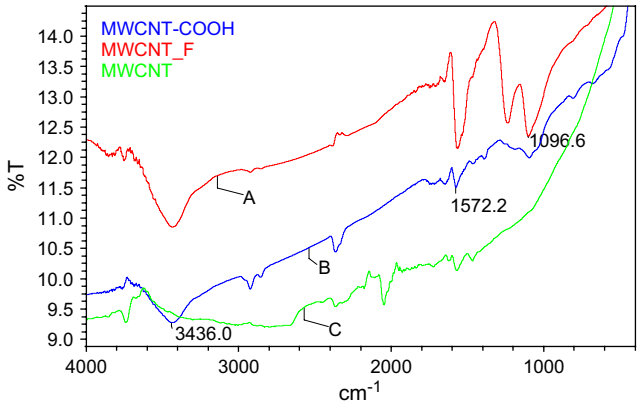


Fig. 2. FT-IR of fluorinated MWCNT (A), carbonyl-modified MWCNT (B) and as received MWCNT (C).

In the second approach we attached fluorine to MWCNT by using a reaction at low temperature and ambient pressure. These conditions are much less drastic than those reported in the literature. The only viable route to direct functionalization of purified CNTs previously reported has been fluorination at elevated temperatures and pressure [5].

The Raman spectra, shown in Fig. 3, show three strong peaks at 1577 $cm^{-1}$, 1309 $cm^{-1}$ and 2621 $cm^{-1}$, corresponding to the typical Raman peaks of carbon nanotubes [24–26]. The peak at 1577 $cm^{-1}$ called G band also characteristic of nanotubes, corresponding to splitting of the $E_{2g}$ mode of graphite is related to the vibration of $sp^2$ bonded carbon atoms in a two dimensional hexagonal lattice. The peak at 1309 $cm^{-1}$ is associated with vibrations of carbon atoms with dangling bonds in-plane terminations of disordered graphite and assigned to residual ill-organized graphite and is called D-band. The peak at 2621 $cm^{-1}$ is assigned to the first overtone of the D mode. The relative intensity of the D-band for modified MWCNTs at 1309 $cm^{-1}$ is significantly increased compare to the D-band for the unmodified MWCNTs. This change is indicative of covalent modification, as it reveals $sp^3$-hybridization or disorder within the nanotube framework. Thus the increase in the relative intensity of the D-band can be attributed to an increased number of $sp^3$-hybridized carbons in the nanotube framework and can be taken as a crude measure of the degree of functionalization.

### 3.2. CNT dispersion and morphology

A schematic of modified carbon nanotube/polymer chemical interactions is shown in Fig. 4. There is a distinct difference in how the modified nanotubes react with the epoxy system (i.e. resin and curing agent). The carboxyl group participates in opening of the epoxide rings, resulting in an ester bond and formation of an OH group [4]. The fluorinated CNT first undergoes a displacement reaction with the amine curing agent [3]. Fluorinated benzyl groups are quite reactive, making such a displacement reaction possible [27]. This results in an amine modified CNT which can essentially act as a curing agent and react with other epoxy groups. This particular

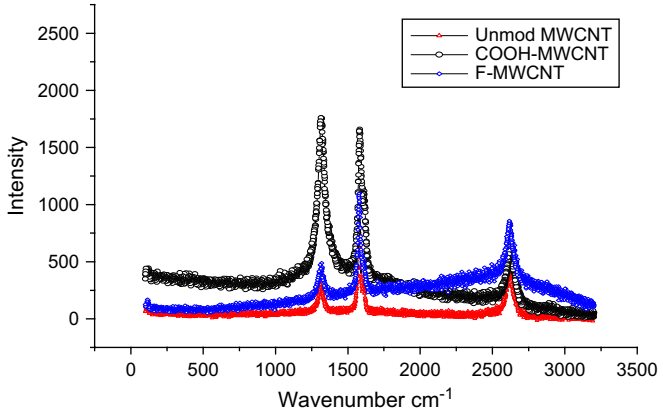


Fig. 3. Raman spectra of carbonyl-modified MWCNT (top curve), fluorinated MWCNT (middle curve), unmodified MWCNT (bottom curve).

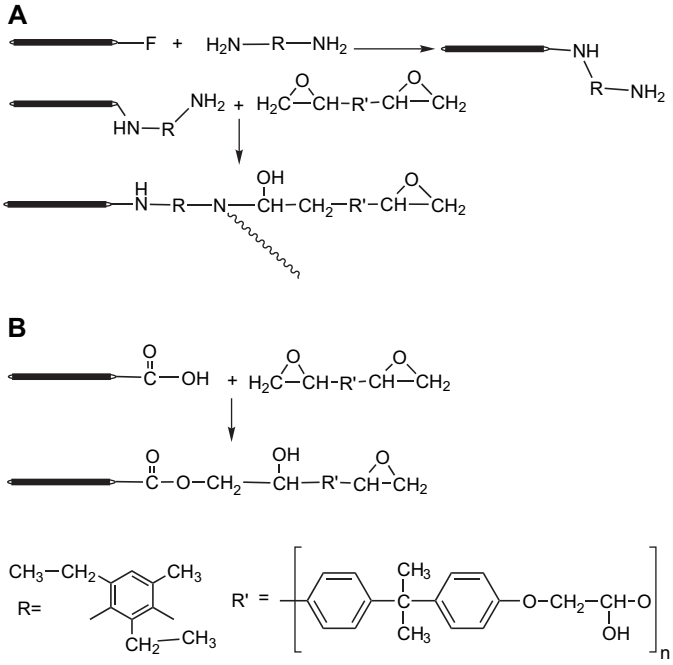


Fig. 4. Schematic of modified CNT reaction with DGEBA resin. (A) Fluorinated CNT reaction with curing agent and DGEBA. (B) Carboxylated CNT reaction with DGEBA resin.

species of modified CNTs can, in principle, leads to a more highly crosslinked structure than that is achievable in COO-modified CNTs. Shearing through the syringe (Fig. 1) results in flow that can be described by Pouiselle's equation (Eq. (1)):

$$\Delta P = \mu L \frac{8Q}{\pi} R^{-4} \tag{1}$$

where $\Delta P$ is the pressure drop, $\mu$ is the viscosity, $Q$ is the volumetric flow rate, $R$ is the orifice radius and $L$ is the length. The shear rate for Newtonian fluids can be described by Eq. (2):

$$\dot{\gamma} = \frac{4Q}{\pi R^3}, \tag{2}$$

where $Q$ is the volumetric flow rate.

For non-Newtonian fluids, the calculated shear rate is an apparent shear rate [28]. We can determine the shear rate by using an experimentally determined volumetric flow rate. Based on an orifice diameter, id of 0.202 cm, and flow rate of 1.5 $cm^3\ s^{-1}$ the calculated shear rate is 1850 $s^{-1}$. A flow study was conducted to correlate the rheological behavior of the fluid to the conditions experienced during flow and the effect on morphology. This was measured by applying a steady shear to the samples.

Figs. 5 and 6 show the viscosity as a function of shear rate for the neat resin and nanocomposites based on the fluorinated and carboxylated MWNTs. The viscosity of the neat resin is independent of the shear rate, consistent with behavior exhibited by a Newtonian fluid. As the nanoparticle content increases, the behavior changes to that of a complex fluid, with shear thinning behavior being exhibited at high shear

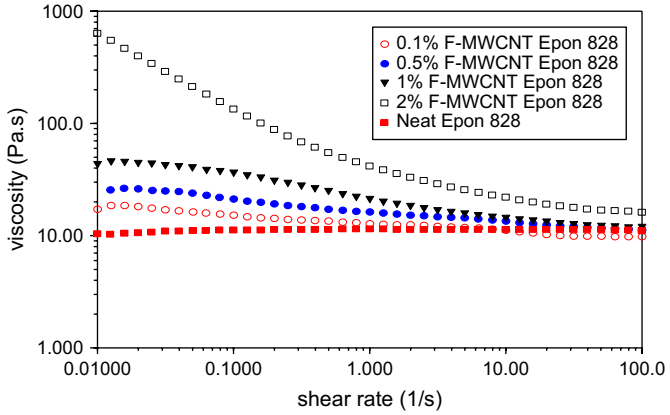


Fig. 5. Viscosity versus shear rate for neat resin and F-CNT nanocomposites. Closed squares are for the neat resin. Open circles are for 0.1% F-CNT nanocomposite. Closed circles are for 0.5% F-CNT nanocomposite. Closed triangles are for 1.0% F-CNT nanocomposite. Open squares are for 2.0% F-CNT nanocomposite.

rates. The low shear rate range is useful for discerning differences in the structure of the systems. As can be seen, the sample with the highest nanotube loading exhibits the highest viscosity in this range. This behavior has been observed for other carbon based nanoparticles dispersed in epoxy resins, including spherical particles and carbon nanotubes [6,16,29]. The effect of surface modification on the flow behavior is examined by overlaying flow curves for nanocomposites containing 1 wt% fluorine and carbonyl groups as shown in Fig. 7. Both systems exhibit higher viscosities than the neat resin. Furthermore, the fluorinated nanocomposite exhibits higher viscosity and a more distinct shear thinning behavior, suggestive of either a more highly dispersed system or stronger resin–nanotube interactions. This is true for all MWNT loadings studied. Kim et al. studied the oscillatory rheology of an epoxy resin dispersed with surface functionalized MWNTs [16]. The MWNTs were functionalized with amines via plasma and wet chemical methods, and carboxylic acid groups. They reported behavior similar to what we observed. It is interesting to note

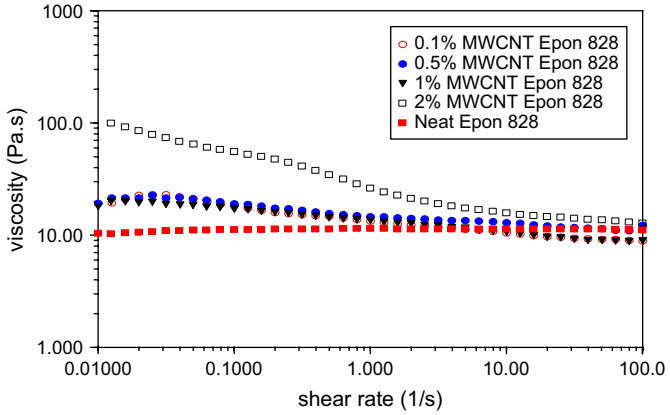


Fig. 6. Viscosity versus shear rate for neat resin and COOH–CNT nanocomposites. Closed squares are for the neat resin. Open circles are for 0.1% CNT nanocomposite. Closed circles are for 0.5% CNT nanocomposite. Closed triangles are for 1.0% CNT nanocomposite. Open squares are for 2.0% CNT nanocomposite.

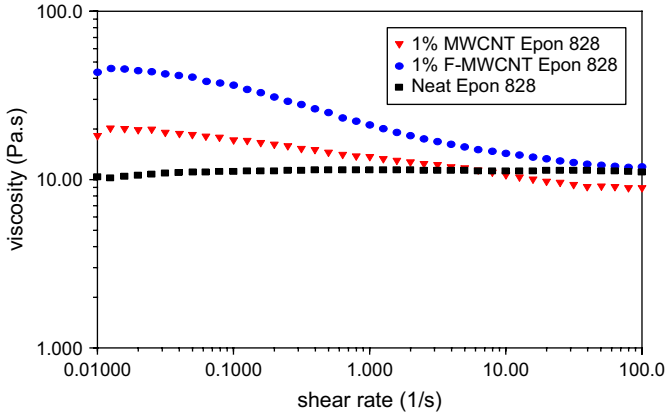


Fig. 7. Viscosity versus shear rate for neat resin and nanocomposites. Closed squares are for the neat resin. Closed circles are for 1.0% F-CNT nanocomposite. Closed triangles are for 1.0% CNT nanocomposite.

that the resin dispersed with the plasma treated MWNTs exhibited the highest viscosity, followed by the acid treated and finally the amine treated MWNTs. The higher viscosity was indicative of stronger interfacial interactions, relative to the other systems. The high viscosity at the low shear rates can be attributed to the formation of a percolated structure by the carbon nanotubes. This structure breaks down as the shear rate increases, resulting in viscosities that are similar at high shear rates for all the systems. These studies suggest that shearing and subsequent curing allows the well dispersed morphology to be locked in before flocculation can occur.

Another positive attribute of the shear device used in our study is the ability to disperse the nanotubes without using a solvent. While solvents can facilitate the dispersal process, incomplete removal of the solvent can result in defective formation as it evaporates during cure, and/or plasticization of the cured polymer, resulting in lowering of the strength and/or $T_g$.

Both TEM and SEM were used to characterize the dispersion and alignment of the nanotubes in the epoxy matrix. Representative micrographs are shown in Fig. 8. The SEM image in Fig. 8a,b shows a fractured surface for an EPON/4_F-CNT sample; a circle is used to highlight some regions in which nanotubes are visible. Fig. 8c shows the dispersion of EPON/4CNT sample. These micrographs (a–c) show a very good dispersion of the nanotubes in the epoxy matrix. The light colored features are the carbon nanotubes. The TEM image in Fig. 8d suggests orientation of the carbon nanotubes, however, quantification is not possible. Raman spectroscopy and wide angle X-ray diffraction can be used to determine the Herman's orientation parameter for carbon nanotubes [30,31], however, Raman spectroscopy is only suitable for single wall nanotubes, and both of these techniques require nanotube concentrations higher than those used in this study.

### 3.3. Viscoelastic and mechanical behavior

#### 3.3.1. Effect of orientation

Fig. 9 shows representative dynamic mechanical scans (using torsion rectangular geometry on AR2000 rheometer)

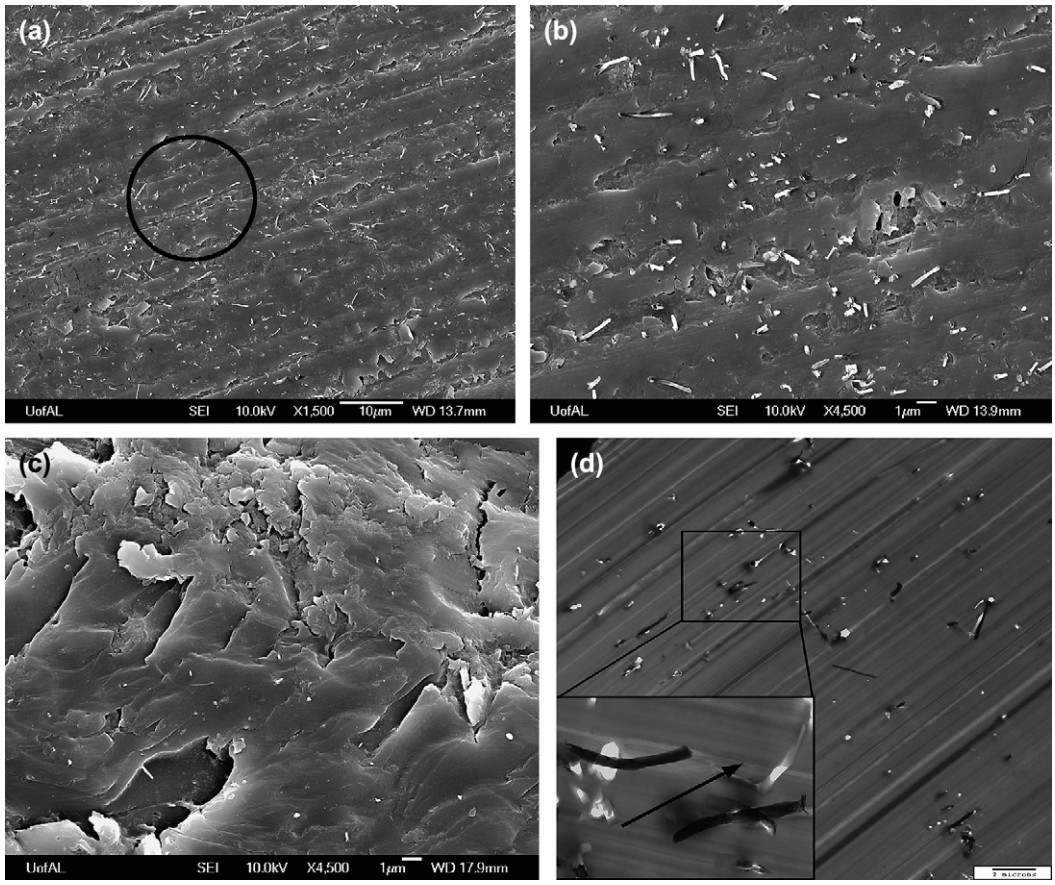


Fig. 8. (a) (b) SEM images of EPON/4_F-CNTPar; (c) SEM images of EPON/4CNTPar and (d) TEM images of EPON/4_F-CNTPar.

for neat epoxy resin, EPON/1CNTPar and EPON/1CNTPer. The samples were prepared by extruding the nanocomposite mixture directly into the mold after multiple mixing iterations. The anisotropy in the modulus is obvious; the modulus parallel to the nanotube axis is 42% higher than that for the neat resin (1.8 GPa vs. 1.0 GPa), and 32% higher than the modulus perpendicular to the nanotube axis (1.8 GPa vs. 1.2 GPa). The

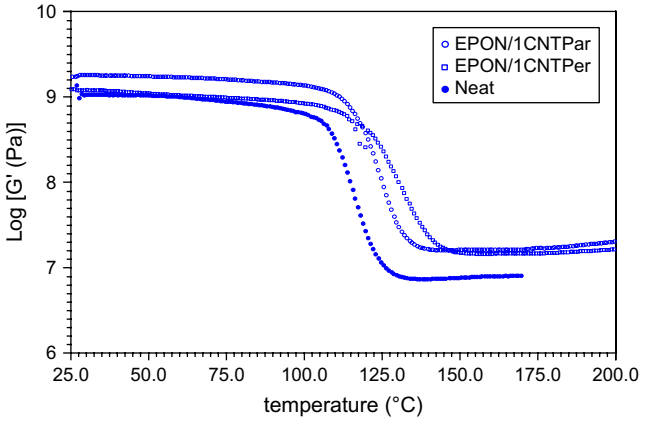


Fig. 9. DMA temperature scans of neat epoxy resin and 1 wt% MWNT samples. Open circles are for the 1% sample tested parallel to nanotube axis. Closed circles are for the neat resin and open squares are for the 1% samples tested perpendicular to nanotube axis.

property enhancements are similar to those reported by others [3,6]. In addition, the rubbery plateau modulus (between 150 °C and 200 °C) is higher by a factor of three for the nanocomposite relative to the neat resin. The $T_g$s increase correspondingly. Several factors may contribute to the increased rubbery plateau modulus including: reinforcing effect by the nanotubes, increased crosslink density and restricted mobility from enhanced polymer–nanotube interactions. Based on composite theories, reinforcement due to relative modulus differences between the nanotubes and the rubbery resin is the most obvious. However, many studies on epoxy/CNT nanocomposites have reported significant glassy modulus enhancements, with no rubbery modulus enhancements [1,2,5,21,32].

It is very difficult to decouple the potential reasons for the rubbery modulus increase. However, if it is assumed that covalent interfacial interactions are increasing the crosslink density, value can be calculated using $\lambda = G/RT$, where $\lambda$ is the crosslink density, for an affine network, $R$ is the universal gas constant and $T$ is the absolute temperature [33]. Affine behavior is characterized by network chains and crosslinks that move proportionately to the macroscopic deformation of the system [28]. Fig. 10 shows crosslink densities, calculated using the plateau modulus measured parallel to the CNT axis. The values of $\lambda$ are similar for both systems, except for the 1 wt% samples, where the F-CNT sample exhibits a higher $\lambda$. This seems to suggest that the mobility restrictions that

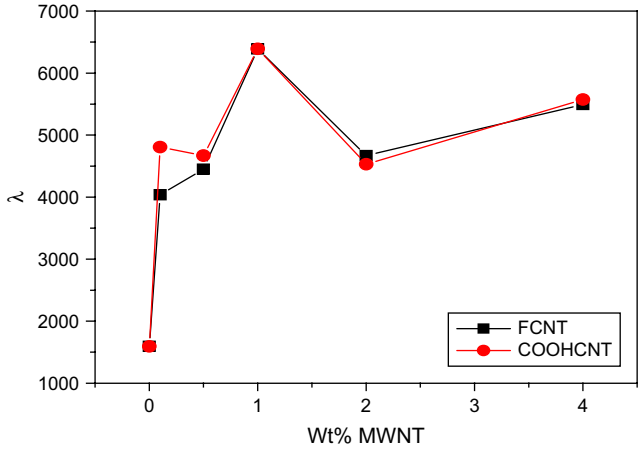


Fig. 10. Crosslink densities for the nanocomposites versus weight percent. Closed squares are for F-CNT nanocomposite. Closed circles are for COOH–CNT nanocomposite.

increase the plateau modulus are due to physical and secondary chemical interactions and not necessarily covalent bond formation. However, based on the chemistry of the crosslinking shown in Fig. 4, the fluorinated CNTs would be expected to give a higher crosslink density when dispersed in the resin and cured. Presumably, variations in the density of functional groups on the CNT surfaces from the two different modification processes are contributing to the behavior observed. This point will be discussed in detail later.

The effect of nanotube orientation on the damping behavior is shown by the plot of tan delta versus temperature in Fig. 11. The height and breadth of the peaks provide additional information about the relaxation behavior of these samples. The height of the peak for the neat resin and sample tested perpendicular to the nanotube axis has similar values of ca. 0.9, while the sample tested parallel to the nanotube axis has a peak value of 0.5, which is nearly one half the magnitude of the peaks for the other samples. This implies that the sample exhibits more

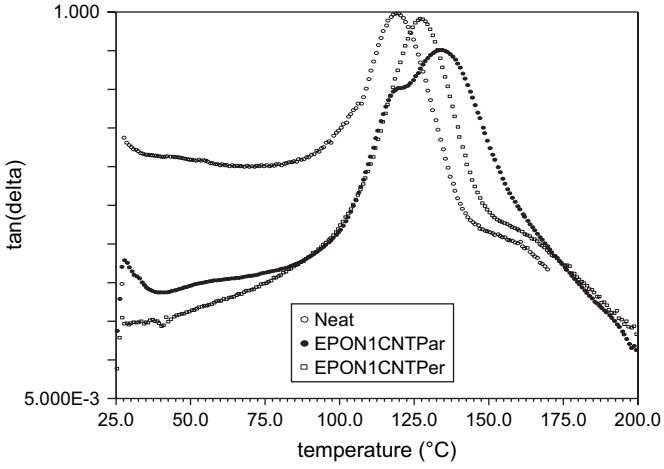


Fig. 11. Tan delta curves of storage modulus versus frequency for neat epoxy resin, and epoxy/CNT nanocomposites. Open circles are for the neat resin. Closed circles are for the 1% sample tested parallel to nanotube axis. Open squares are for the 1% samples tested perpendicular to nanotube axis.

elastic behavior when tested in the direction of the nanotubes, and less elastic behavior when tested in the direction in which the resin dominates the response. The significant increase in breadth of the peak for the sample tested parallel to the nanotube axis suggests a broader distribution of relaxation times, presumably due to more nanotube–polymer interactions, and hence restricted mobility.

### 3.3.2. Effect of interfacial chemistry

Varying the nanotube surface chemistry has a similar effect, as shown in Fig. 12, which plots the storage modulus and tan delta for the neat resin and 1 wt% nanocomposites. This composition was chosen because it represents a good balance between surface functional group concentration and MWNT loading. Remaining discussions will center on samples with this nanotube concentration, tested parallel to the nanotube axis. The value of $G'$ in the transition region is useful for discerning differences in the temperature scans. In addition to an enhancement in glassy modulus with surface modification, the modulus at 125 °C ranges from 10 to 190 to 480 MPa for the neat, carboxylated and fluorinated systems, respectively. This

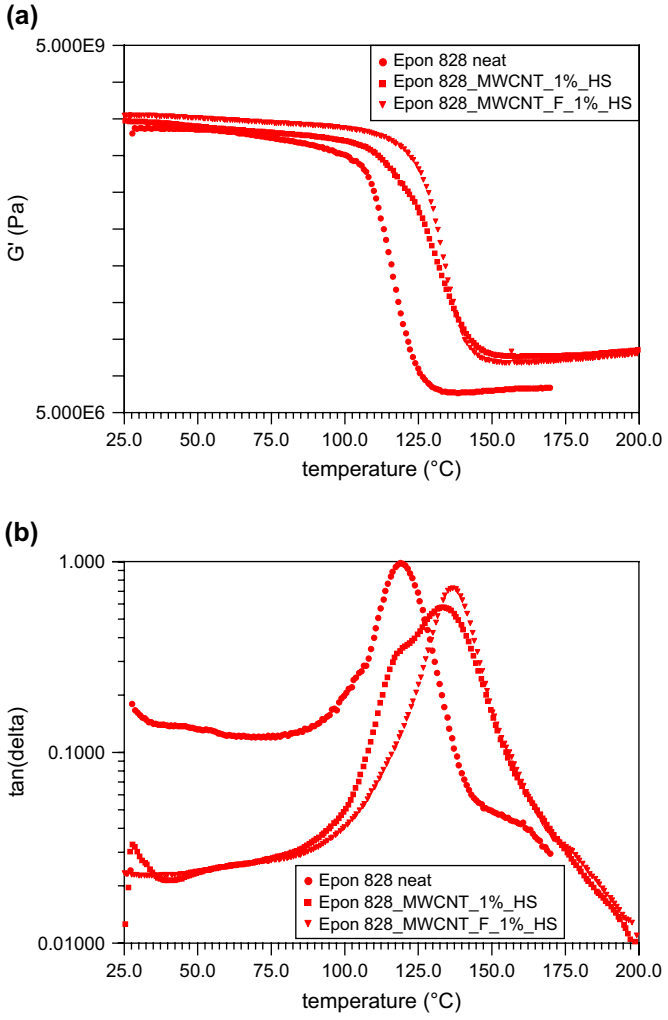


Fig. 12. Storage modulus (a) and tan delta (b) versus temperature for neat resin and 1 wt% nanocomposites.

very striking difference results from the higher reactivity of the fluorinated MWNTs and/or their high propensity for crosslinking compared to the carboxylated MWNTs resulting in a distinctly different crosslink topology. The $T_g$s for these systems are 119 °C, 130 °C and 137 °C for the neat, carboxylated and fluorinated systems, respectively. These findings are corroborated by the tan delta curves, which show magnitudes of 0.9, 0.6 and 0.84 for the neat, carboxylated and fluorinated systems, respectively. For the same samples, the peak width at half height for the carboxylated sample is twice that for the neat resin and 1.6 times that for the fluorinated sample. The extremely broad relaxation for the carboxylated system has a low temperature shoulder. The relaxation behavior observed for this sample is likely caused by heterogeneity in the MWNT dispersion. This could lead to a physical partitioning effect, in which the CNTs disrupt the local resin/curing agent stoichiometry. Variations in the concentration of reactive groups on the nanotube surface can also affect the way the crosslink forms, and hence the relaxation behavior. These issues are currently being investigated further.

In order to further characterize the relaxation behavior of neat resin and nanocomposites, a series of isothermal frequency sweeps were conducted from 75 °C to 200 °C, and used to construct master curves, using time–temperature superposition, t-T-s. Time–temperature superposition is based on the fact that the viscoelastic behavior at one temperature can be related to that at another temperature by a change in the time or frequency scale only [34,35]. For dynamic mechanical data, this implies that by selecting a reference temperature, one can shift higher temperature curves to lower frequencies and lower temperature curves to higher frequencies, thereby constructing a master curve. Thus, the master curve covers a much wider range of frequencies than those experimentally accessible.

Representative master curves for samples tested parallel to the CNT axis are shown in Fig. 13. Typical viscoelastic behavior is observed. Moving from highest frequency to lowest, modulus is the highest at very high frequencies, followed by a transition region, and a rubbery plateau at the lowest

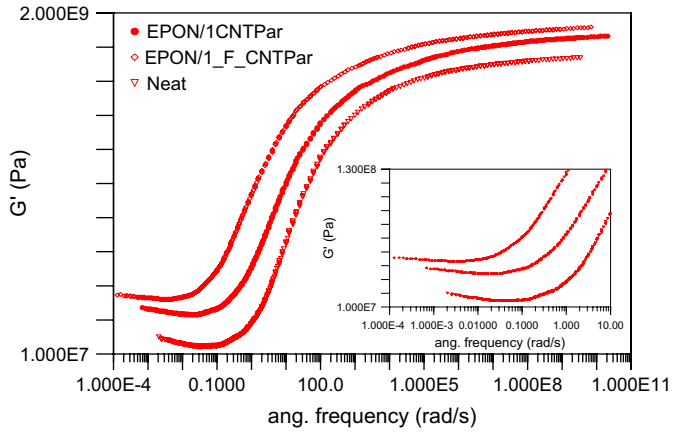


Fig. 13. Master curves of storage modulus versus frequency for neat epoxy resin, and epoxy/CNT nanocomposites.

frequencies, which is shown in the inset. The highest glassy modulus (at 100 MHz) is observed for EPON/1_F-CNTPar; the value is 1.5 GPa compared to 1.3 GPa for EPON/1CNTPar and 0.94 GPa for the neat resin. This corresponds to an increase of 40% for the EPON/1_F-CNTPar and 30% for the EPON/1_COOH–CNTPar relative to the neat resin, and is similar to values reported by others [3,6]. At a frequency of 1 Hz, which corresponds to the frequency used in the temperature scans shown in Fig. 13, the highest modulus is observed for the EPON/1_F-CNTPar sample, followed by the EPON/1CNTPar and finally the neat resin. This suggests that the 1_F-CNT sample has a longer relaxation time, which correlates with the higher $T_g$ observed for this sample. Activation energies associated with this $T_g$ were calculated from Arrhenius plots of the shift factors. The values for the activation energies are 251 KJ mol$^{-1}$, 317 KJ mol$^{-1}$ and 398 KJ mol$^{-1}$ for the neat resin, EPON/1CNTPar and EPON/1_F-CNTPar, respectively. These findings suggest that a stronger interaction exists between the fluorine groups and the epoxy resin, relative to that between the carboxylated nanotube and epoxy resin.

Additional differences in the relaxation behavior are most easily discerned at the lower frequencies. An inset of this region is shown in Fig. 13, which plots the plateau modulus as a function of CNT surface modifications. The increase in plateau modulus with CNT loading is caused by a reduction in chain mobility brought about by CNT–resin interactions, as discussed for the temperature scans. The nature of the interactions (i.e. whether they are primary or secondary) is not clear. However, some recent studies have shown that both carboxyl and fluorine modified nanotubes form primary bonds with epoxy resin systems. Based on the reaction schematic shown in Fig. 4, samples containing the fluorinated CNTs are expected to form a more highly crosslinked structure, however, differences in the nanotube structure and modifier concentration may have a significant effect on the plateau modulus, $T_g$ and activation energy. For example, the carbonyl-CNTs were modified by oxidizing in a strong acid. This acid may have decreased the length of the nanotubes, leading to a higher concentration of carbonyl groups on the surface, relative to that of the fluorine modified nanotubes. Precise control of nanotube modification parameters, including functional group, density of groups on the surface and location of groups on the surface is an area of intense investigation. In addition, variation in the physical characteristics of nanotube, including diameter, length distribution and chirality (especially for single wall nanotubes) may also have an effect on how the nanotubes are modified and subsequently interact with the polymeric host. These issues are currently being investigated.

## 4. Conclusions

Successful integration of surface modified CNTs into thermoset polymers is most effectively accomplished via covalent bonds between the two. In addition to enhancing dispersability of the CNTs into the thermoset, formation of covalent bonds has a dramatic effect on the behavior of the thermoset resin, in both the uncured and cured state. For example, in the

uncured state, the presence and nature of the covalent bond affects the rheological behavior, resulting in a transition from Newtonian behavior for the neat resin to non-Newtonian behavior for the nanocomposites. This effect is more prevalent for the nanocomposite based on fluorinated nanotubes. The high shear rates experienced during dispersal help to deaggregate the nanotubes, and the well dispersed structure is locked in by curing. In the solid state the nature of the covalent interactions dramatically affects the glassy modulus, $T_g$ relaxation (and activation energies associated with it) as well as the rubbery plateau modulus. For example, the 1 wt% carbonyl-modified sample exhibits a low temperature shoulder in its tan delta peak. Furthermore, the peak width at half height for the carboxylated sample is twice that for the neat resin and 1.6 times that for the fluorinated sample. These effects suggest heterogeneity in the crosslink topology, which possibly stems from variations in the nanotube surface coverage. In addition to the effects listed above, the order for the activation energy associated with the relaxations is fluorinated> carboxylated>neat resin, which agrees with the structure–property correlations expected. Studies on the effect of the surface modifications on cure behavior and crosslink formation are underway.

## Acknowledgement

This work was funded by NSF DMR (Grant no. 0404278).

## References

[1] Gong X, Liu J, Baskaran S, Voise RD, Young JS. Surfactant-assisted processing of carbon nanotube/polymer composites. Chem Mater 2000; 12(4):1049–52.
[2] Liao Y-H, Marietta-Tondin O, Liang Z, Zhang C, Wang B. Investigation of the dispersion process of SWNTs/SC-15 epoxy resin nanocomposites. Mater Sci Eng A 2004;385(1–2):175–81.
[3] Zhu J, Kim J, Peng H, Margrave JL, Khabashesku VN, Barrera EV. Improving the dispersion and integration of single-walled carbon nanotubes in epoxy composites through functionalization. Nano Lett 2003;3(8): 1107–13.
[4] Eitan A, Jiang K, Dukes D, Andrews R, Schadler LS. Surface modification of multiwalled carbon nanotubes: toward the tailoring of the interface in polymer composites. Chem Mater 2003;15(16):3198–201.
[5] Zhu J, Peng H, Rodriguez-Macias F, Margrave JL, Khabashesku VN, Imam AM, et al. Reinforcing epoxy polymer composites through covalent integration of functionalized nanotubes. Adv Funct Mater 2004; 14(7):643–8.
[6] Song YS, Youn JR. Influence of dispersion states of carbon nanotubes on physical properties of epoxy nanocomposites. Carbon 2005;43(7): 1378–85.
[7] Sandler J, Shaffer MSP, Prasse T, Bauhofer W, Schulte K, Windle AH. Development of a dispersion process for carbon nanotubes in an epoxy matrix and the resulting electrical properties. Polymer 1999;40(21): 5967–71.
[8] Moniruzzaman M, Winey KI. Polymer nanocomposites containing carbon nanotubes. Macromolecules 2006;39(16):5194–205.
[9] Thostenson ET, Ren Z, Chou T-W. Advances in the science and technology of carbon nanotubes and their composites: a review. Compos Sci Technol 2001;61(13):1899–912.
[10] Xie X-L, Mai Y-W, Zhou X-P. Dispersion and alignment of carbon nanotubes in polymer matrix: a review. Mater Sci Eng R 2005;49(4):89–112.
[11] Hussain F, Hojjati M, Okamoto M, Gorga RE. Review article: polymer-matrix nanocomposites, processing, manufacturing, and application: an overview. J Compos Mater 2006;40(17):1511–75.
[12] Fan Z, Advani SG. Characterization of orientation state of carbon nanotubes in shear flow. Polymer 2005;46(14):5232–40.
[13] McCarthy B, Coleman JN, Czerw R, Dalton AB, Byrne HJ, Tekleab D, et al. Complex nano-assemblies of polymers and carbon nanotubes. Nanotechnology 2001;12(3):187–90.
[14] Bahr JL, Yang J, Kosynkin DV, Bronikowski MJ, Smalley RE, Tour JM. Functionalization of carbon nanotubes by electrochemical reduction of aryl diazonium salts: a bucky paper electrode. J Am Chem Soc 2001;123(27):6536–42.
[15] Liu P. Modifications of carbon nanotubes with polymers. Eur Polym J 2005;41(11):2693–703.
[16] Kim JA, Seong DG, Kang TJ, Youn JR. Effects of surface modification on rheological and mechanical properties of CNT/epoxy composites. Carbon 2006;44(10):1898–905.
[17] Yaping Z, Aibo Z, Qinghua C, Jiaoxia Z, Rongchang N. Functionalized effect on carbon nanotube/epoxy nano-composites. Mater Sci Eng A 2006;435–436:145–9.
[18] Wang S, Liang Z, Liu T, Wang B, Zhang C. Effective amino-functionalization of carbon nanotubes for reinforcing epoxy polymer composites. Nanotechnology 2006;17(6):1551–7.
[19] Rinzler AG, Liu J, Dai H, Nikolaev P, Huffman CB, Rodríguez-Macías FJ, et al. Large-scale purification of single-wall carbon nanotubes: process, product, and characterization. Appl Phys A Mater Sci Process 1998;67(1):29–37.
[20] Shelimov KB, Esenaliev RO, Rinzler AG, Huffman CB, Smalley RE. Purification of single-wall carbon nanotubes by ultrasonically assisted filtration. Chem Phys Lett 1998;282(5–6):429–34.
[21] Gojny FH, Nastalczyk J, Roslaniec Z, Schulte K. Surface modified multi-walled carbon nanotubes in CNT/epoxy-composites. Chem Phys Lett 2003;370(5–6):820–4.
[22] Chen RJ, Zhang Y, Wang D, Dai H. Noncovalent sidewall functionalization of single-walled carbon nanotubes for protein immobilization. J Am Chem Soc 2001;123(16):3838–9.
[23] Chen J, Hamon MA, Hu H, Chen Y, Rao AM, Eklund PC, et al. Solution properties of single-walled carbon nanotubes. Science 1998;282(5386): 95–8.
[24] Belin T, Epron F. Characterization methods of carbon nanotubes: a review. Mater Sci Eng B 2005;119(2):105–18.
[25] Mitchell CA, Bahr JL, Arepalli S, Tour JM, Krishnamoorti R. Dispersion of functionalized carbon nanotubes in polystyrene. Macromolecules 2002;35(23):8825–30.
[26] Bahr JL, Tour JM. Highly functionalized carbon nanotubes using in situ generated diazonium compounds. Chem Mater 2001;13(11):3823–4.
[27] Smith MB. Organic synthesis. 2nd ed. New York: McGraw-Hill; 1946.
[28] MacOsko CW. Rheology: principles, measurements, and applications. 1st ed. New York: John Wiley & Sons Inc; 1994.
[29] Kotsilkova R, Fragiadakis D, Pissis P. Reinforcement effect of carbon nanofillers in an epoxy resin system: rheology, molecular dynamics, and mechanical studies. J Polym Sci Part B Polym Phys 2005;43(5): 522–33.
[30] Camponeschi E, Florkowski B, Vance R, Garrett G, Garmestani H, Tannenbaum R. Uniform directional alignment of single-walled carbon nanotubes in viscous polymer flow. Langmuir 2006;22(4):1858–62.
[31] Jose MV, Dean D, Tyner J, Price G, Nyairo E. Polypropylene/carbon nanotube nanocomposite fibers: process–morphology–property relationships. J Appl Polym Sci 2007;3844–50.
[32] Miyagawa H, Drzal LT. Thermo-physical and impact properties of epoxy nanocomposites reinforced by single-wall carbon nanotubes. Polymer 2004;45(15):5163–70.
[33] Rubinstein M, Colby RH. Polymer physics. 1st ed. New York: Oxford University Press; 1956.
[34] Williams ML, Landel RF, Ferry JD. J Am Chem Soc 1955;77:3701–7.
[35] Woicke N, Keuerleber M, Hegemann B, Eyerer P. Three-dimensional thermorheological behavior of isotactic polypropylene across glass transition temperature. J Appl Polym Sci 2004;94(3):877–80.